

Parameter estimation of coalescing supermassive black hole binaries with LISA

K.G. Arun^{1,*}

¹*Raman Research Institute, Bangalore 560 080, India*

(Dated: February 8, 2020)

Laser Interferometer Space Antenna (LISA) will routinely observe coalescences of supermassive black hole (BH) binaries up to very high redshifts. LISA can measure mass parameters of such coalescences to a relative accuracy of $10^{-4} - 10^{-6}$, for sources at a distance of 3 Gpc. The problem of parameter estimation of massive nonspinning binary black holes using post-Newtonian (PN) phasing formula is studied in the context of LISA. Specifically, the performance of the 3.5PN templates is compared against its 2PN counterpart. The improvement due to the higher order corrections to the phasing formula is examined by calculating the errors in the estimation of mass parameters, angular resolution and the luminosity distance. The estimation of the mass parameters \mathcal{M} and η are significantly enhanced by using the 3.5PN waveform instead of the 2PN one. The estimation of angular resolution and distance show very little improvement. For an equal mass binary of $2 \times 10^6 M_\odot$ at a luminosity distance of 3 Gpc, the improvement in chirp mass is $\sim 8\%$ and that of η is $\sim 40\%$. Estimation of coalescence time t_c shows negligible variation with PN orders. The improvement is larger for the unequal mass binary mergers. Chirp mass and η are improved by $\sim 18\%$ and 63% , respectively, for a $10M_\odot$ BH inspiralling into a $10^6 M_\odot$ supermassive black hole. The parameter estimation using a single detector of LISA is compared against the case where LISA is considered to be a two detector network. For a binary of $2 \times 10^6 M_\odot$ the error in estimation of mass parameters using two detector network is improved by about 40% in comparison with the one detector case. The distance and angular resolution is improved by about 90% and 70% respectively.

PACS numbers: 04.30.Db, 04.25.Nx, 04.80.Nn, 95.55.Ym

I. INTRODUCTION

Most of our near-by galaxies harbour supermassive black holes (BH) at their centre [1]. If this is the case, then merger of such galaxies would produce a binary system composing of two supermassive BHs. Simulations indicate that there could be primordial supermassive BH binaries at the centres of the first galaxies [2]. An understanding of the formation and evolution of these binaries is very important from the view point of cosmology and structure formation. Many of these binaries coalesce under gravitational wave (GW) radiation reaction within Hubble time. Supermassive BH binaries in the mass range $10^4 - 10^7 M_\odot$ will emit gravitational waves (GW) of frequency $10^{-4} - 10^{-1}$ Hz during its adiabatic inspiral phase which can be observed by the proposed space-borne GW missions such as LISA [3, 4] with high (\sim a few thousands) signal to noise ratio (SNR) up to very high redshifts (~ 10).

Different authors have investigated the implications of these observations in the context of astrophysics, cosmology and testing general relativity and its alternatives. LISA observations of BH coalescences can be used to study the growth of BHs as the universe evolved and for mapping the distribution of BHs as function of the redshift [5, 6, 7]. LISA will be able to measure luminosity distances to the sources with an accuracy $\sim 1 - 10\%$. If the redshift associated with the event is known by electromagnetic observations, these sources can be used as very high precision standard candles and to study the distance-redshift relation [8, 9]. Ref [10] discussed the potential of LISA to observe binaries containing a BH in the intermediate mass regime ($\sim 10^3 M_\odot$) and use it as a probe of strong field aspects of gravity.

LISA could probe many strong gravitational field effects which are not possible to explore with other observational means. Both inspiral and ring-down GW signals can be used for this. Refs [11, 12] studied the possibility of using the quasi-normal mode oscillations to test the no-hair theorem of general relativity since these modes will be characterized *only* by the mass and angular momentum of the BH (in general relativity). Hughes and Menou examined another possibility [13] if LISA detects both inspiral and ring-down signals from the same source. By measuring the total mass independently from both the signals one can estimate the mass difference which will be the mass-energy lost due to GWs. They suggested that an extension of this idea including spin effects could in principle test the BH area theorem. Further, inspiral of a stellar mass BH into a SMBH will be another interesting source for LISA using which many properties of the central SMBH can be probed including the possibility to map the spacetime following the geodesics of the stellar mass BH (See e.g.[14, 15]) and measuring the multipole moments of the spacetime.

*Electronic address: arun@rri.res.in

LISA will provide an unique opportunity to test general relativity and its alternatives. Will and his co-workers have discussed the potential of LISA to test general relativity as well as its alternatives like Brans-Dicke theory and massive graviton theories [16, 17]. Recently this issue was discussed in a more realistic scenario of spinning binaries using 2PN phasing [6, 7]. Blanchet and Sathyaprakash proposed another test based on post-Newtonian (PN) GW phasing formula by measuring the 1.5PN GW tail effect and showing how it can be used as a test of general relativity [18, 19]. This proposal was recently generalized to higher order terms in the phasing formula by Arun *et al* and it was argued that such a test would allow one to probe the nonlinear structure of gravity [20, 21].

A very accurate parameter extraction scheme is central to performing all these analyses. A parameter estimation scheme based on matched filtering, similar to that for the ground based detectors such as LIGO and VIRGO, will be employed for LISA also. An efficient matched filtering would in turn demand a very accurate model of the gravitational waveform. In order to compute the gravitational waveform from a compact binary system, one solves the two-body problem in general relativity perturbatively using different approximation schemes since no exact solutions for this problem exist till date. The final waveform can be expressed as a post-Newtonian expansion which is a power series in v/c where v is the gauge independent velocity parameter characterising the source (See Ref. [22] for an exhaustive review on the formalism). In our notation $\frac{v}{c}$ refers to half a PN order.

Since the information about the phase is more important for the process of matched filtering, one uses a simplified model of the inspiral waveform (the so called restricted waveform) where phase is modelled to a high PN order retaining the Newtonian amplitude. In doing so, one is neglecting the effect of other harmonics [23, 24] in the amplitude of the wave and also the higher order PN corrections to the dominant harmonic at twice the orbital frequency. In the present study, we deal only with the restricted waveform in the Fourier domain obtained using stationary phase approximation. The phasing formula for nonspinning binaries, is presently complete up to 3.5PN order [25, 26, 27].

The implications of the higher PN order phasing in the context of parameter estimation problem has been investigated by different authors. Based on the framework set up by Refs [28, 29], Cutler and Flanagan [30] investigated the importance of the 1.5PN phasing formula [31]. Effect of including spin-orbit coupling parameter, at 1.5PN order, into the space of parameters was one of interesting issues addressed. Two independent works by Krolak *et al.* [32] and Poisson and Will [33] analysed the problem of parameter estimation using the 2PN phasing formula of Ref. [25]. Inclusion of the 2PN spin-spin coupling term at 2PN and its effect on errors of other parameters was the focus of their analysis.

Recently Arun *et al.* [34] investigated the effect of the 2.5, 3 and 3.5PN terms for the parameter estimation of nonspinning binaries (a similar work was carried out independently by Berti and Buonanno [35]). Using covariance matrix calculations, they inferred that by employing the 3.5PN phasing instead of the 2PN one, the improvement in estimation of errors in chirp mass and symmetric mass ratio can be as high as 19% and 52% respectively for the ground based detectors such as LIGO and VIRGO.

Cutler was the first to address the problem of parameter estimation in the LISA context [36]. He used the 1.5PN waveform including the spin-orbit effect and studied the estimation of errors associated with the mass parameters as well as distance and angular resolution of the binary. Seto investigated the effect of finite arm length of LISA using 1.5PN phasing [37]. Vecchio revisited the parameter estimation with the 1.5PN waveform [38] where he used the waveform for circular orbit but with “simple precession” (as opposed to non-precessing case of [36]) and examined the implications of it for the estimation of distance and angular resolution. Various aspects of the 2PN parameter estimation, such as the spin-spin coupling, was investigated by different authors [5, 6, 7]. Ref [6] studied the effect of spin terms in testing alternate theories of gravity with the LISA observations. Refs [5, 7] also addressed the issue of mapping the merger history of massive BHs using LISA observations in the 2PN context. While all these calculations are within the restricted waveform approximation where the PN corrections to the amplitude is completely neglected, there are investigations about the effect of including these amplitude corrections in the context of parameter estimation [39, 40, 41, 42].

In the present work we extend these analyses to the inspirals of supermassive BH binaries for the LISA. Coalescences of BHs of masses $10^4 - 10^7 M_\odot$ at a luminosity distance of 3 Gpc are considered. We assume LISA will observe these events for one year duration. Using the 3.5PN phasing we calculate the errors associated with the estimation of the mass parameters, distance and angular resolution and compare against the corresponding 2PN results. We also study the effect of orbital motion for parameter estimation by comparing these results with the other two cases, one where LISA pattern functions are not used and another when LISA is considered to be a two detector network instead of a single Michelson interferometer.

The rest of the paper is organized as follows. Sec. II discusses all the necessary inputs required for the paper such as a brief introduction to parameter estimation using covariance matrix, noise model for LISA, model for the waveform and some other conventions followed in the paper. Sec III discusses the main results and their implications and Sec IV provides the summary and future directions.

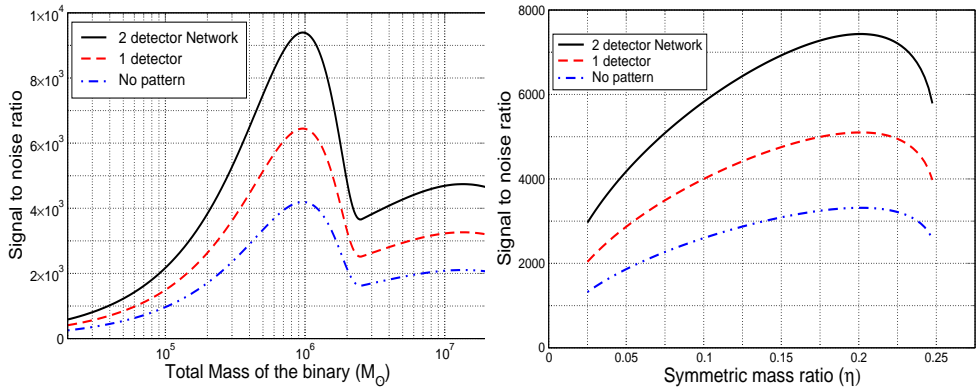


FIG. 1: Left hand panel: Variation of signal-to-noise ratio with the total observed mass for the 3 cases: First by ignoring the pattern functions (Case A), second including pattern functions but considering LISA to be one interferometer (Case B) and the third one considering LISA to be a two detector network (Case C). Right hand panel: Variation of SNR with η for a binary whose with one of the constituent mass of $10^6 M_\odot$. Sources are assumed to be optimally oriented. For the last two cases, we have assumed an integration time of one year for the signal.

II. PARAMETER ESTIMATION FOR LISA WITH 3.5PN PHASING

A. Parameter estimation using the covariance matrix

We summarize the theory of parameter estimation in the context of Gaussian random detector noise, addressed in the GW context first by Finn and Chernoff [28, 29] and implemented by Cutler and Flanagan [30]. Let us assume an inspiral GW signal is detected meeting the necessary detection criteria and one needs to extract the intrinsic and extrinsic parameters from the signal by matched filtering.

For sources like inspiralling compact binaries, where a prior source modelling is possible to predict the gravitational waveform, *matched filtering* is an ideal method both for detection as well as parameter estimation of the signal [43]. In matched filtering, the detector output is filtered using a bank of theoretical templates with different signal parameters. The parameters of the template which obtains the best signal-to-noise ratio (SNR) gives the “measured” values of the signal parameters. These values, in general, will be different from the “actual” values due to the presence of noise. The problem of parameter estimation addresses the question of how close are the measured values to the actual ones and what the associated errors are in the estimation of different parameters. For a given signal, different realizations of noise lead to different sets of best-fit parameters of the signal. When the background noise is a stationary, random, Gaussian process, at high enough SNRs the best-fit values of the parameters have a Gaussian distribution centered around the actual values of the parameters.

If λ^i denotes the actual value of the parameters and $\lambda^i + \Delta\lambda^i$, the measured value, then the root mean square difference $\Delta\lambda^i$ obeys a Gaussian distribution: $p(\Delta\lambda_i) \propto \exp(-\Gamma_{ij}\Delta\lambda^i\Delta\lambda^j/2)$ where Γ_{ij} is the Fisher information matrix constructed from Fourier domain representation of the waveform is given by

$$\Gamma_{ij} = 2 \int_{f_{\text{in}}}^{f_{\text{fin}}} \frac{\tilde{h}_i^*(f)\tilde{h}_j(f) + \tilde{h}_i(f)\tilde{h}_j^*(f)}{S_h(f)} df. \quad (2.1)$$

Here, $\tilde{h}_i(f) := \partial\tilde{h}(f)/\partial\lambda^i$, $\tilde{h}(f)$ is the Fourier domain gravitational waveform and $S_h(f)$ is the (one-sided) noise power spectral density of the detector. It also follows that the root-mean-square errors are given by $\sigma^i = \sqrt{\Sigma^{ii}}$, where $\Sigma = \Gamma^{-1}$ is called the *covariance matrix* and σ_i is the root mean square error in measuring λ^i . The non-diagonal elements of the covariance matrix can be used to define the correlation coefficient between two parameters: $c^{ij} = \frac{\Sigma^{ij}}{\sqrt{\Sigma^{ii}\Sigma^{jj}}}$. Repeated indices are *not* summed over in the above expressions. Finally the SNR can be expressed in terms of the Fourier domain signal $\tilde{h}(f)$ as

$$\rho^2 = 4 \int_{f_{\text{in}}}^{f_{\text{fin}}} \frac{|\tilde{h}(f)|^2}{S_h(f)} df. \quad (2.2)$$

In the present case our λ^i denoting the set of parameters are given by $\{t_c, \phi_c, \mathcal{M}, \eta, D_L, \bar{\phi}_S, \bar{\phi}_L, \bar{\theta}_S, \bar{\theta}_L\}$. In the case where pattern functions are not included the above set reduces to $\{t_c, \phi_c, \mathcal{M}, \eta\}$. The additional elements of the

parameter set denotes the distance, orientations and locations of the source in the sky specified with respect to the fixed solar system based coordinate system.

Other than the covariance matrix approach, which is valid only in the high SNR limit, there have been proposals in literature addressing the parameter estimation problem using Monte-Carlo methods. In Ref [44], the authors compared the error estimates obtained using the covariance matrix with the Monte-Carlo simulations. Recently another parameter estimation scheme based on Bayesian statistics using Markov chain Monte-Carlo method also has been proposed and implemented [45, 46].

In the above integrals, the upper limit of integration is $f_{\text{fin}} = \text{Min}[f_{\text{iso}}, f_{\text{end}}]$, where f_{iso} is the frequency of the innermost stable circular orbit for the test particle case, $f_{\text{iso}} = (6^{3/2} \pi m)^{-1}$ and f_{upper} corresponds to the upper cut-off of the LISA noise curve $f_{\text{end}} = 1\text{Hz}$. We have chosen the lower limit of frequency $f_{\text{in}} = \text{Max}[f_{\text{in}}, f_{\text{lower}}]$ where f_{in} is calculated by assuming the signal to last for one year in the LISA sensitivity band and f_{lower} , the low frequency cut-off for LISA noise curve, is assumed to be 10^{-5}Hz^1 .

B. Model for the LISA noise curve

We follow the noise model of LISA as given in Ref [6] which is a slightly modified version of [47]. The noise spectral density consists of a non-sky averaged part [47] and confusion noise due to the galactic and extra galactic white dwarf binaries [47, 48, 49]. The total instrumental plus confusion noise reads as

$$S_h(f) = \min \left\{ \frac{S_h^{\text{NSA}}(f)}{\exp(-\kappa T_{\text{mission}}^{-1} dN/df)}, S_h^{\text{NSA}}(f) + S_h^{\text{gal}}(f) \right\} + S_h^{\text{ex-gal}}(f). \quad (2.3)$$

$$S_h^{\text{NSA}}(f) = \left[9.18 \times 10^{-52} \left(\frac{f}{1\text{ Hz}} \right)^{-4} + 1.59 \times 10^{-41} + 9.18 \times 10^{-38} \left(\frac{f}{1\text{ Hz}} \right)^2 \right] \text{ Hz}^{-1}, \quad (2.4a)$$

$$S_h^{\text{gal}}(f) = 2.1 \times 10^{-45} \left(\frac{f}{1\text{ Hz}} \right)^{-7/3} \text{ Hz}^{-1}, \quad (2.4b)$$

$$S_h^{\text{ex-gal}}(f) = 4.2 \times 10^{-47} \left(\frac{f}{1\text{ Hz}} \right)^{-7/3} \text{ Hz}^{-1}, \quad (2.4c)$$

$$\frac{dN}{df} = 2 \times 10^{-3} \text{ Hz}^{-1} \left(\frac{1\text{ Hz}}{f} \right)^{11/3}, \quad (2.4d)$$

where T_{mission} is the duration of LISA mission. See Sec II C of Ref [6] for a detailed summary.

C. LISA detector configuration and the waveform model

LISA is a three-arm interferometer where each arm has a length of $5 \times 10^6\text{ km}$. These arms form an equilateral triangle and move in a heliocentric orbit with a 20° lag to the earth and the plane of the detector tilted at 60° with respect to the ecliptic (See [3, 36] for details). LISA with three arms is essentially equivalent to a pair of two-arm detectors. We consider two cases: one where we assume the estimation of mass parameters is not affected because of their correlations with the angular variables and second when we estimate the associated errors with angular variables and luminosity distance of the source. Since the information about the angular variables are encoded in the so-called pattern functions which describes the orbital motion of LISA, in the first case we use a waveform which is averaged over the pattern functions. In the second case, we do not average over the pattern functions and use the information from the LISA orbital motion to discuss the estimation of angular resolution and luminosity distance to the source. Further, in the second case we consider cases when (i) LISA is a single two arm-detector and (ii) as a two detector network in order to understand the effect of network configuration for parameter estimation. The LISA antenna

¹ Another way of choosing the limits of integration is to calculate the time over which the signal will last once it enters the LISA band. See [5] for example, where the duration of the signal is calculated using the expression for $t(f)$. It assumes $f_{\text{lower}} = 10^{-4}\text{Hz}$ and 3 year mission time for LISA.

patterns, describing its orbital motion, is given in [36] which is used for the present study (also see Appendix A of Ref [6] for these expressions).

Unlike the ground based detectors where the two arms have an angle 90° , the LISA arms are at 60° . As shown by Cutler [36], the relative strain amplitude (which is the gravitational waveform) in the LISA case can be simply be related to the 90° interferometer case by multiplying the latter by a factor $\sqrt{3}/2$. Using this input, the Fourier domain waveform within the stationary phase approximation can be written down as [6, 36]

$$\tilde{h}_\alpha(f) = \frac{\sqrt{3}}{2} \mathcal{A} f^{-7/6} e^{i\psi(f)}, \quad \alpha = \text{I, II}, \quad (2.5)$$

$$\mathcal{A} = \frac{1}{\sqrt{30\pi^{2/3}}} \frac{\mathcal{M}^{5/6}}{D_L}, \quad (2.6)$$

where α labels the interferometer, f the GW frequency and \mathcal{M} , the chirp mass which is related to total mass $m = m_1 + m_2$ and symmetric mass ratio $\eta = m_1 m_2 / m^2$ by $\mathcal{M} = \eta^{3/5} m$. Luminosity distance to the source is denoted by D_L . The GW phase $\psi(f)$ appearing in the formula is completed up to 3.5PN [26, 27, 50] and its Fourier domain representation is given in [51, 52]. We find it more convenient to write it as

$$\psi(f) = 2\pi f t_c - \phi_c + \sum_{k=0}^{k=7} \alpha_k v^k, \quad (2.7)$$

where $v = (\pi m f)^{1/3}$ is the PN variable which is related to gauge independent source velocity in system of units where $G = 1 = c$ which we follow henceforth in the paper. Eq (3.4) of [34] gives the α_k for different values of $k = 0 \dots 7$.

In the case where we do not average the pattern functions, the waveform can be written as [6]

$$\tilde{h}_\alpha(f) = \frac{\sqrt{3}}{2} \mathcal{A} f^{-7/6} e^{i\Psi(f)} \left\{ \frac{5}{4} \tilde{A}_\alpha(t(f)) \right\} e^{-i(\varphi_{p,\alpha}(t(f)) + \varphi_D(t(f)))}, \quad (2.8)$$

where $\varphi_{p,\alpha}(t(f))$ and $\varphi_D(t(f))$ are the polarization phase and Doppler phase respectively [36]. $\tilde{A}_\alpha(t(f))$ correspond to the amplitude modulations induced by the LISA's orbital motion. $\tilde{A}_\alpha(t(f))$ and $\varphi_{p,\alpha}(t(f))$ depends on the pattern functions $F_+^\alpha(t)$ and $F_\times^\alpha(t)$ and hence vary with time. For the explicit expressions for $\varphi_{p,\alpha}$ and φ_D , we refer the readers to Refs [6, 36]. For 3.5PN accurate expression for $t(f)$ we use the following relation

$$2\pi t(f) = \frac{d\psi(f)}{df}. \quad (2.9)$$

This can be rewritten as

$$t(f) = t_c - \sum_{k=0}^7 t_k^v v^k, \quad (2.10)$$

and values of t_k^v is given in Refs [51, 52] which can readily be used.

For calculations where LISA is assumed to be a two detector network, we calculate the SNR and Fisher matrix using

$$\rho^{\text{Network}} = \sqrt{\rho_{\text{I}}^2 + \rho_{\text{II}}^2}, \quad (2.11)$$

$$\Gamma_{ab}^{\text{Network}} = \Gamma_{ab}^{\text{I}} + \Gamma_{ab}^{\text{II}}. \quad (2.12)$$

The errors for the two detector case are obtained inverting the total Fisher matrix following the procedure outlined in Sec. II A.

Throughout the paper we assume a cosmological model with zero spatial curvature ($\Omega_\kappa = 0$, $\Omega_\Lambda + \Omega_M = 1$) and Hubble's constant to be $H_0 = 70 \text{ km s}^{-1} \text{ Mpc}^{-1}$. The luminosity distance is given by

$$D_L = \frac{1+z}{H_0} \int_0^z \frac{dz'}{[\Omega_M(1+z')^3 + \Omega_\Lambda]^{1/2}}, \quad (2.13)$$

where z denotes the redshift of the source.

We calculate the Fisher matrix for the different configurations of LISA using the corresponding waveforms and invert it to get the covariance matrix. The elements of the covariance matrix are used for discussing the errors and correlation coefficients of different parameters in the next section. While discussing the trends with the PN orders, its useful to keep in mind that apart from the usual phase $\psi(f)$, there are additional PN serieses of $t(f)$ both in the amplitude and phase when pattern functions are included, which can influence the results.

III. RESULTS AND DISCUSSIONS

For convenience of later discussion we introduce the following notation for the three detector configurations we deal with: Case A, where the pattern functions are not included, or in other words, orbital motion of LISA is not considered; Case B where pattern functions are included and LISA is considered to be a single interferometer and finally Case C, where LISA is considered to be a two interferometer network. Though consideration of Case A is basically to check our codes with earlier results at 2PN by [6] and to compare the LISA results with those of the ground based detectors [34], it also enables us to compare and contrast the parameter estimation features when pattern functions are included. For the last two cases we assume a signal integration time of one year.

Before discussing the results for parameter estimation for different configurations of LISA, it is instructive to examine how the SNR varies with the mass for these configurations. As a check of our codes, we have reproduced the results in Table V of Ref. [6]. Left panel of Fig 1 compares the variation of SNR with the observed total mass of the system for the three cases of our interest. As expected the highest SNR for any chosen system is for the case of the two detector network (Case C). It is almost 50% higher than the single interferometer case (Case B), which in turn is better by about 50% than the case when pattern functions are not used (Case A). The noise curve has maximum SNR for sources whose observed mass is $10^6 M_\odot$. The source is assumed to be at a luminosity distance of 3 Gpc and optimally oriented². The trends reported here are independent of the values of these angles chosen.

A. Parameter estimation of equal mass binaries with the 3.5PN phasing

We discuss the performance of the 3.5PN restricted waveform from the parameter estimation point of view for the three different cases mentioned above. Our aim is to study the variation of errors in different parameters with the total observed mass³ of the binary for different PN orders and different detector configurations. This would not only give us an idea of the improvement brought in by the use of higher order phasing but also about the convergence of the PN series for the problem of parameter estimation. We have checked our codes by reproducing the results of Ref [36] at 1.5PN (with their models for the noise and the signal) and at 2PN with that in Table III and V of Ref [6] for the nonspinning case. The important results of our study are discussed in detail in what follows. The errors in estimation of different parameters for a $2 \times 10^6 M_\odot$ binary at 3 Gpc is provided in Table I for different PN orders in the phasing.

1. Improvement in estimation of mass parameters

We plot in Fig. 2 the variation with mass of the errors in chirp mass and η for different PN orders for Case C. There is significant improvement in the estimation by the use of 3.5PN phasing instead of the 2PN one especially for more massive systems. For a prototypical system of a binary BH each of mass $10^6 M_\odot$, we find that the chirp mass and η improve by 8% and 39% respectively. They are similar to the results for the ground based detectors as discussed in [34] but at an entirely different mass range. Inclusion of pattern functions does not affect the improvement in the mass parameters. For a typical binary, LISA will be able to measure chirp mass with an incredibly small fractional accuracy of 2×10^{-6} and η by about 5×10^{-5} .

Variation with mass: The chirp mass worsens with increase in total mass of the binary whereas the estimation of η improves initially and then decreases. These effects can be understood as follows. When the total mass increases there are two competing effects in action: the increase in errors with mass, since signal lasts for smaller duration, and the variation of SNR with mass as in Fig 1 which is a characteristic of the noise curve. For chirp mass the errors increase so rapidly that the variation in SNR does not affect the trend and the errors continue increase monotonically with mass. For η , there is trade-off between these two competing effects which accounts for the minima in the curve.

² Following Cutler [36], we have chosen the orientation of the binary to be $\bar{\mu}_S = 0.9$, $\bar{\phi}_S = 2$, $\bar{\mu}_L = -0.8$, $\bar{\phi}_L = 5.0$, where $\bar{\mu}_S = \cos \bar{\theta}_S$ and $\bar{\mu}_L = \cos \bar{\theta}_L$.

³ By total mass, we always refer to the total redshifted mass $m'(1+z)$, where m' is the actual source mass and z is the redshift of the source. This is the mass that is observed by the GW observations.

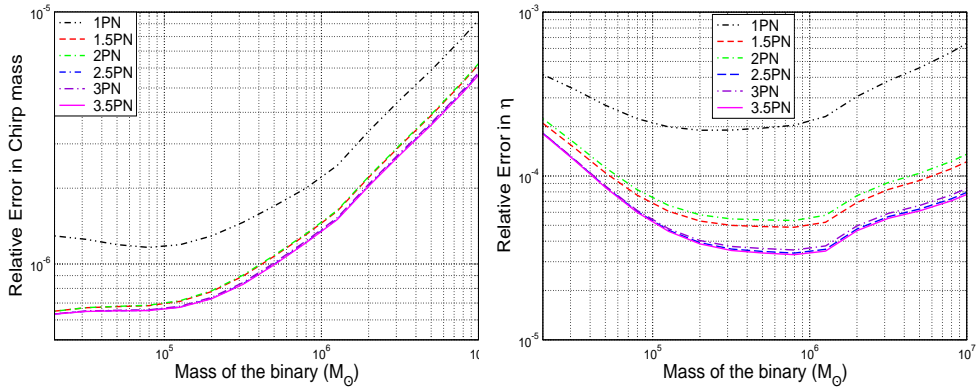


FIG. 2: Variation of errors with the total observed mass for different PN order restricted waveforms for LISA with pattern functions for the two detector network configuration. The convergence of the results is evident in both the cases. Sources are assumed to be at 3 Gpc.

2. Errors in coalescence time

Measuring the time of coalescence of a binary system is important to carry out electro-magnetic observation of the event associated with the binary merger. We discuss the trends in estimation of t_c below.

In the absence of pattern functions, the errors in t_c show trends similar to that of [34], *i.e.*, with increase in PN order, the errors oscillate in a sense opposite to the mass parameters and in going from 2PN to 3.5PN there is a net degradation in its estimation which is about 43% for the prototypical system considered. This was explained in Ref [34] based on the correlations between t_c , \mathcal{M} and η . It was noticed that *both* $c_{\mathcal{M}t_c}$ and $c_{\eta t_c}$ are positive and follows the same trend as the error in t_c . Increase in these correlations implied a worsened estimation of t_c .

By including the pattern functions, for Cases B and C, the trends are quite different. The variation of errors in t_c with mass for different PN orders are presented in the left hand panel of Fig. 3. As evident from the plot and Table I, there is no significant improvement or degradation of errors from 2PN to 3.5PN up to a total mass of about $5 \times 10^6 M_\odot$. Beyond that, parameter estimation worsens similar to Case A. At $2 \times 10^7 M_\odot$, the degradation is $\sim 32\%$ for Case C.

In order to understand this, we examine the correlation coefficients in these two mass regimes. In the regime where there is little change in errors at higher PN orders, $c_{t_c \mathcal{M}}$ is positive but $c_{t_c \eta}$ is negative whereas for the high mass end, $c_{t_c \eta}$ flips its sign and similar to Case A, both are positive and there is net degradation in the estimation. This could be a consequence of orbital modulations of LISA suppressing the PN oscillations in errors seen when pattern functions are used. Towards the higher mass end, because of the smaller duration of the signal, the modulations may be less effective and the PN oscillations could reappear.

3. Post-Newtonian convergence in the parameter estimation context

Since PN series is an asymptotic series, the rate of convergence of the results is a very important issue for detection as well as parameter estimation. We use the word ‘convergence’ to mean that the difference (in errors) between two consecutive PN orders is smaller as we go to higher orders considered. As remarked in Refs. [30, 33], if the parameter estimation scheme is based on lower order (2PN) phasing, the systematic errors due to the absence of higher order terms may be more than the statistical errors caused by the noise. Since we study here the implications of 3.5PN phasing, we examine the convergence of the series based on our results for different PN orders.

As Fig 2 would reveal, though there will be improvement by using 3.5PN phasing instead of the 2PN one, most of the improvement comes from the transition from 2PN to 2.5PN and after that the series continues to show its characteristic oscillatory behaviour, but rather slowly, suggesting that phasing at orders higher than 3.5PN may not cause much improvement. But curiously the situation is different for the unequal mass case which is discussed in Sec III C.

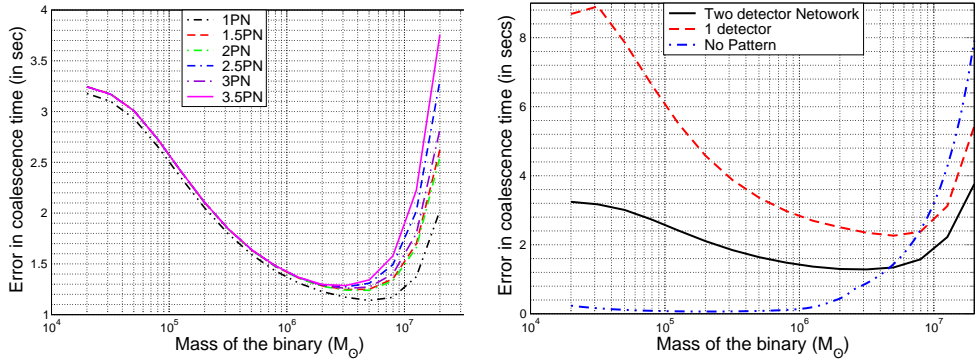


FIG. 3: Errors in t_c for sources at 3 Gpc for different PN orders (left panel) and comparison of the three detector configurations (right panel).

4. Comparison of different detector configurations

We compare the estimation of errors with different detection configurations now. While comparing different detector configurations there are two factors which play important roles. One is the dimensionality of the parameter space, increase of which will cause an increase in the errors and second is the contribution from the SNR corresponding to each configuration increase of which improves the estimation. For Case A, since there are no pattern dependent parameters, the total parameter space is essentially 4 dimensional, the parameters being, $t_c, \phi_c, \mathcal{M}, \eta$. When we make a transition to Case B, where new parameters corresponding to the distance to the source and its location and orientation are added to the space of parameters and the parameter space is now 9 dimensional: $t_c, \phi_c, \mathcal{M}, \eta, D_L, \bar{\mu}_L, \bar{\mu}_S, \bar{\phi}_L, \bar{\phi}_S$. This increase in dimensionality of the space will cause increase in errors of the earlier parameters. Because of the introduction of pattern functions there is an increase in SNR as well. The final errors, in comparison with Case A, will depend on whether the rise in SNR sufficiently compensates for the increase in the errors of different parameters. Case C will have the additional advantage of the two detector configuration, which modifies the SNR and the Fisher matrix (and hence the errors), while comparing with Case A, though the increased dimensionality causes worsening of errors of the mass parameters and t_c in this case also.

Fig 4 compares the measurement accuracies of the three configurations under consideration. It may seem surprising at first sight that the estimation of chirp mass for Case B is larger than that for Case A, whereas it is much smaller for Case C. A careful examination will reveal the reason. When one transits from the case without pattern functions to the one detector case including pattern functions, the dimensionality of the parameter space is increased. Though the new configuration provides larger SNR, this is not sufficient for the error in estimation of \mathcal{M} to be less than that of Case A. Since for η the errors do not worsen as much as \mathcal{M} because of the introduction of new parameters, the increase in SNR pushes the estimation to a level better than Case A. But for total mass less than $10^4 M_\odot$, errors in η is larger for Case B compared to Case A. The network configuration significantly reduces the errors for \mathcal{M} and η by 46% and 37%, respectively, compared to the one interferometer case. This is because both SNR and Fisher matrix are modified by the presence of the second detector and hence errors are smaller than the other two cases.

The right hand panel of Fig 3 compares the three detector configurations for the estimation of t_c . This can also be understood by the argument given above. Up to a total mass of $\sim 10^7 M_\odot$, Case A has the smallest errors. But beyond this point, the higher SNR of the other two configurations lead to better estimation and the network configuration has the smallest errors.

5. Parameter estimation and Number of GW cycles

In Ref. [34], the correlation between the improvement in errors across different PN orders and the number of total and useful GW cycles [53] was studied. It was found that though they are good indicators of how the errors at each order vary with the total mass of the system, they alone cannot explain the variation of errors across different PN orders in the context of ground based detectors. We confirm this feature in the LISA context. By comparing the number of GW cycles for different PN orders (and for the mass range considered here) with the errors in estimation of parameters we see that neither the magnitude of the errors nor their oscillations correlate with the trends in number of cycles. Irrespective of whether the total number of GW cycles is very high ($\sim 10^5$) (as in the case of LISA) or low (\sim hundreds) (as for the ground based detectors) the PN trends in parameter estimation are too complicated to be

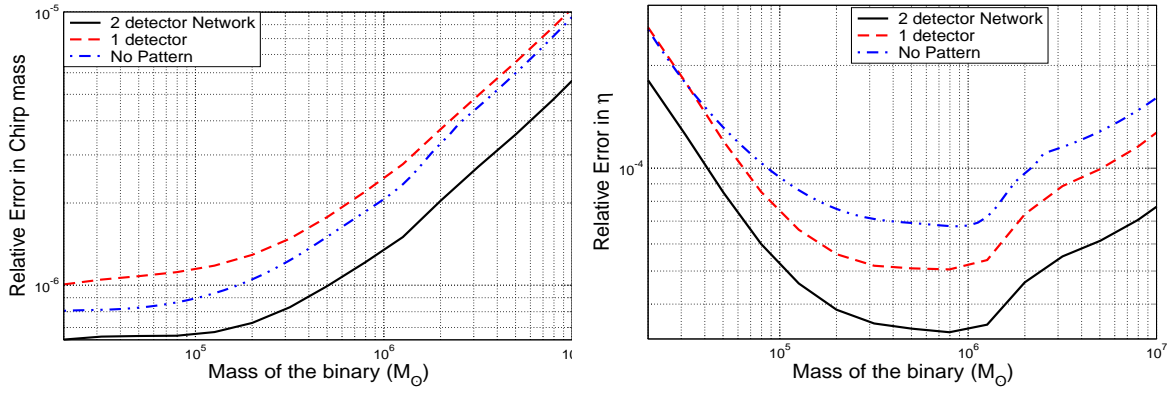


FIG. 4: Errors in \mathcal{M} and η for sources at 3 Gpc for the three cases considered. There is significant improvement in measuring the parameters because of the orbital motion of LISA and using it as a 2 detector network.

explained solely in terms of this. However the variation of errors with mass can be understood on the basis of number of the cycles and variation in SNR (again, not in terms of only one of them).

TABLE I: Variation of errors in different parameters with PN order for the two detector network configuration of LISA. The system considered is a binary of mass $2 \times 10^6 M_\odot$ at a luminosity distance of 3 Gpc. Δt_c is in seconds and $\Delta \Omega_S$ is in steradians.

PN Order	Δt_c (sec)	$\Delta \mathcal{M}/\mathcal{M}$ (10^{-6})	$\Delta \eta/\eta$ (10^{-5})	$\frac{\Delta D_L}{D_L}$	$\Delta \Omega_S$ (10^{-5} str)
1PN	1.227	3.367	30.56	0.0858	3.782
1.5PN	1.284	2.206	6.886	0.0902	4.071
2PN	1.280	2.225	7.587	0.0899	4.051
2.5PN	1.294	2.048	4.744	0.0904	4.077
3PN	1.288	2.075	4.960	0.0903	4.072
3.5PN	1.298	2.037	4.635	0.0904	4.072

B. Estimation of distance and angular resolution for equal mass binaries

Because of the orbital motion of LISA, one can determine the luminosity distance and angular resolution of the source using the one interferometer configuration of LISA. We discuss below the accuracy with which LISA can measure the luminosity distance and angular resolution for a single interferometer configuration as well as a two detector network. Error in angular resolution is defined in terms of the angular variables $\bar{\theta}_S$ and $\bar{\phi}_S$ as

$$\Delta \Omega_S = 2\pi |\sin \bar{\theta}_S| \left\{ \Sigma_{\bar{\theta}_S \bar{\theta}_S} \Sigma_{\bar{\phi}_S \bar{\phi}_S} - \Sigma_{\bar{\theta}_S \bar{\phi}_S}^2 \right\}^{1/2}, \quad (3.1)$$

where Σ_{ij} denotes the elements of the covariance matrix. Similar studies were carried out in Ref [6, 36] for spinning binaries but using the 1.5PN and 2PN phasings respectively.

The estimation of distance and angular resolution is not improved much because of the additional phasing terms. This is not surprising, since the additional terms in the phasing formula do not carry any information about location or orientation of the binary. One may need to go beyond the restricted waveform model of the waveform in order to achieve this. Some preliminary studies in this regard [39, 40, 41, 42, 54, 55] do suggest the same. Going beyond the restricted waveform approximation would mean including the amplitude corrections to the waveform from the two GW polarizations, currently completed up to 2.5PN order [23, 24]. This is because the amplitude terms are functions also of the angular positions of the source in the sky, introduction of which could break different degeneracies, allowing better parameter estimation [39, 40].

In Fig 5 we present the variation of errors in luminosity distance and angular resolution with total observed mass. The effect of using LISA as a network is quite obvious in this case, as errors drop significantly by using the network

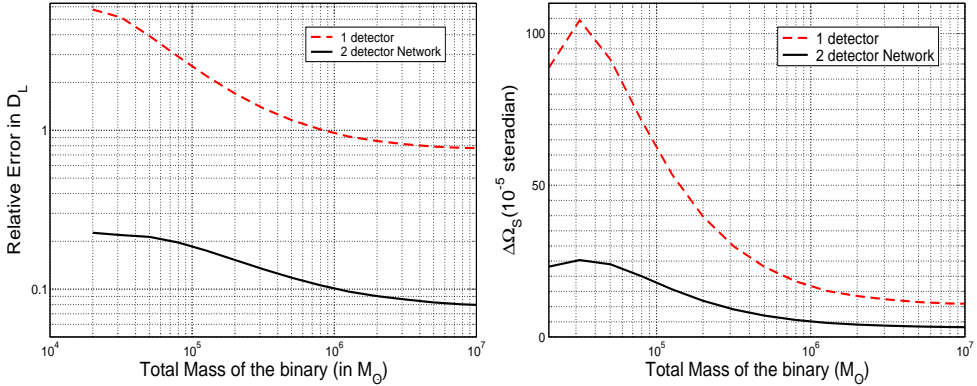


FIG. 5: Errors in estimation of distance and angular resolution for sources at 3 Gpc for the single detector and detector network cases considered. Network configuration significantly improves the parameter estimation.

configuration. Using the network, the luminosity distance estimation is better by 88% and angular resolution improves by 70% for a $2 \times 10^6 M_\odot$ binary.

C. Parameter estimation for unequal mass binaries

Lastly we perform a similar analysis for unequal mass systems where $\eta < 0.25$. Variation in SNR of such systems with η is presented in the right hand panel of Fig 1. For this case a BH of $10M_\odot$ inspiralling into a MBH of $10^6 M_\odot$ constitutes our prototypical system. We find that the improvement due to the inclusion of higher order terms are more dominant here than for equal mass binary case. For the prototypical system considered above, we find an improvement of 18% for chirp mass and 63% for η for the case of the two detector network.

This larger improvement for the unequal mass binaries is not a special feature of the LISA noise curve; for the ground based detectors also a similar feature exists. But unlike in the LISA case, where many such unequal mass binaries are astrophysically plausible, for the ground based detectors such sources are not prototypical.

For LISA, inspirals with very small mass ratio (often called as extreme mass ratio inspirals (EMRIs)), are very important sources. For EMRI's the spin effects and orbital eccentricity play a very important role. Since the present study is for non-spinning binaries, a detailed study with the spin and eccentricity terms for the test particle case is necessary before drawing any solid conclusions. However, our analysis seems to suggest that one may need to use higher order phasing formula in order to get convergent results for the unequal mass case. We postpone a detailed study of the problem to the future.

IV. SUMMARY AND FUTURE WORKS

The significance of higher order phasing terms is investigated in the LISA case for different configurations. Using the 3.5PN inspiral waveform instead of the 2PN one, which is currently employed in the GW experiments, mass parameters can be estimated with improved precision for LISA. For the case of LISA the estimation of source location and orientation is not improved significantly by the use of the restricted 3.5PN template. One may need to go beyond the restricted waveform approximation in order to achieve it. Especially, implications of the full waveform with the 2.5PN polarizations of Ref [24] together with the 3.5PN phasing of [26] would be an interesting exercise to carry out. The PN series shows convergent behaviour, beyond 2.5PN order. Compared to the LISA one detector configuration, the two detector network improves the parameter estimation substantially. The distance estimation is improved by 88% and that of angular resolution by 70%. Mass parameters register an improvement of $\sim 40\%$ due to the network. The number of GW cycles is a good indicator of how the errors vary with mass but not across different PN orders. The improvement in parameter estimation is more pronounced for binaries with unequal masses. The problem of unequal mass binaries should be revisited with the inclusion of spin effects to higher orders as spin effects play a dominant role in the dynamics of such systems. However our results may be an indicator of the trends for the extreme mass ratio inspirals which will be observed by LISA. One would like to address this problem with specific attention to the extreme mass ratio case in the future. Finally, inclusion of the spin effects at 2.5PN order in the phase [56] would help us go beyond the results of [6] for the spinning case and will be exciting especially for the equal mass case.

The very high accuracy parameter extraction possible with LISA will make it a useful tool of astrophysics and provide thorough probes of strong field aspects of gravity in the future.

Acknowledgments

The author thanks B R Iyer for useful discussions, valuable comments on the manuscript and constant encouragement. Conversations with B S Sathyaprakash on issues related the parameter estimation with LISA and his encouragement to pursue this problem are gratefully acknowledged. The author is grateful to Sanjeev Dhurandhar for discussions and comments on the manuscript. The author also thanks M S S Qusailah for useful discussions.

All the calculations reported in this paper are performed with *Mathematica*.

[1] D. Richstone, E. A. Ajhar, R. Bender, G. Bower, A. Dressler, S. M. Faber, A. V. Filippenko, K. Gebhardt, R. Green, L. C. Ho, et al., *Nature* **395**, A14 (1998), astro-ph/9810378.

[2] B. Volker and L. Abraham, *The Astrophysical Journal* **596**, 34 (2003), astro-ph/0212400.

[3] P. L. Bender, *Lisa: Laser interferometer space antenna for the detection and observation of gravitational waves: Pre-phase: A report* (1995), unpublished.

[4] K. Danzmann, *Class. Quantum Grav.* **14**, 1399 (1997).

[5] S. A. Hughes, *Mon. Not. R. Astron. Soc.* **331**, 805 (2002), astro-ph/0108483.

[6] E. Berti, A. Buonanno, and C. M. Will, *Phys. Rev. D* **71**, 084025 (2005), gr-qc/0411129.

[7] E. Berti, A. Buonanno, and C. M. Will, *Class. Quant. Grav.* **22**, S943 (2005), gr-qc/0504017.

[8] B. F. Schutz, *Nature (London)* **323**, 310 (1986).

[9] D. E. Holz and S. A. Hughes, *Astrophys. J.* **629**, 15 (2005), astro-ph/0504616.

[10] M. C. Miller, *The Astrophysical Journal* **618**, 426 (2005), astro-ph/0409331.

[11] O. Dreyer, B. Kelly, B. Krishnan, L. S. Finn, D. Garrison, and R. Lopez-Aleman, *Class. Quantum Grav.* **21**, 787 (2004), gr-qc/0309007.

[12] E. Berti, V. Cardoso, and C. M. Will, *Phys. Rev. D* (2005), gr-qc/0512160.

[13] S. A. Hughes and K. Menou, *Astrophys. J.* **623**, 689 (2005), astro-ph/0410148.

[14] F. Ryan, *Phys. Rev. D* **56**, 1845 (1997).

[15] N. A. Collins and S. A. Hughes, *Physical Review D* **69**, 124022 (2004), gr-qc/0402063.

[16] C. M. Will, *Phys. Rev. D* **57**, 2061 (1998), gr-qc/9709011.

[17] C. M. Will and N. Yunes, *Class. Quantum Grav.* **21**, 4367 (2004), gr-qc/0403100.

[18] L. Blanchet and B. S. Sathyaprakash, *Class. Quant. Grav.* **11**, 2807 (1994).

[19] L. Blanchet and B. S. Sathyaprakash, *Phys. Rev. Lett.* **74**, 1067 (1995).

[20] K. G. Arun, B. R. Iyer, M. S. S. Qusailah, and Sathyaprakash, *Class. Quantum Grav.* **23**, L37 (2006), gr-qc/0604018.

[21] K. G. Arun, B. R. Iyer, M. S. S. Qusailah, and Sathyaprakash (2006), (submitted), gr-qc/0604067.

[22] L. Blanchet, *Living Rev. Rel.* **5**, 3 (2002), gr-qc/0202016.

[23] L. Blanchet, B. R. Iyer, C. M. Will, and A. G. Wiseman, *Class. Quant. Grav.* **13**, 575 (1996), gr-qc/9602024.

[24] K. G. Arun, L. Blanchet, B. R. Iyer, and M. S. Qusailah, *Class. Quant. Grav.* **21**, 3771 (2004), erratum-*ibid.* **22**, 3115 (2005), gr-qc/0404185.

[25] L. Blanchet, T. Damour, B. R. Iyer, C. M. Will, and A. G. Wiseman, *Phys. Rev. Lett.* **74**, 3515 (1995), gr-qc/9501027.

[26] L. Blanchet, G. Faye, B. R. Iyer, and B. Joguet, *Phys. Rev. D* **65**, 061501(R) (2002), Erratum *Phys. Rev. D* **71**, 129902(E) (2005), gr-qc/0105099.

[27] L. Blanchet, T. Damour, G. Esposito-Farèse, and B. R. Iyer, *Phys. Rev. Lett.* **93**, 091101 (2004), gr-qc/0406012.

[28] L. Finn, *Phys. Rev. D* **46**, 5236 (1992).

[29] L. Finn and D. Chernoff, *Phys. Rev. D* **47**, 2198 (1993).

[30] C. Cutler and E. Flanagan, *Phys. Rev. D* **49**, 2658 (1994).

[31] C. Cutler, T. Apostolatos, L. Bildsten, L. Finn, E. Flanagan, D. Kennefick, D. Markovic, A. Ori, E. Poisson, G. Sussman, et al., *Phys. Rev. Lett.* **70**, 2984 (1993).

[32] A. Krolak, K. Kokkotas, and G. Schäfer, *Phys. Rev. D* **52**, 2089 (1995).

[33] E. Poisson and C. Will, *Phys. Rev. D* **52**, 848 (1995).

[34] K. G. Arun, B. R. Iyer, B. S. Sathyaprakash, and P. A. Sundararajan, *Phys. Rev. D* **71**, 084008 (2005), erratum-*ibid. D* **72**, 069903 (2005), gr-qc/0411146.

[35] E. Berti and A. Buonanno (2004), unpublished.

[36] C. Cutler, *Phys. Rev. D* **57**, 7089 (1998).

[37] N. Seto, *Physical Review D* **66**, 122001 (2002), gr-qc/0210028.

[38] A. Vecchio, *Phys. Rev. D* **70**, 042001 (2004).

[39] T. A. Moore and R. W. Hellings, *Phys. Rev. D* **65**, 062001 (2002).

[40] R. W. Hellings and T. A. Moore, *Class. Quant. Grav.* **20**, S181 (2002), gr-qc/0207102.

- [41] A. M. Sintes and A. Vecchio (2000), gr-qc/0005058.
- [42] A. M. Sintes and A. Vecchio (2000), gr-qc/0005059.
- [43] L. A. Wainstein and V. D. Zubakov, *Extraction of Signals from Noise* (Prentice-Hall, Englewood Cliffs, 1962).
- [44] R. Balasubramanian, B. S. Sathyaprakash, and S. V. Dhurandhar, Phys. Rev. D **53**, 3033 (1996), erratum-ibid. D **54**, 1860, gr-qc/9508011.
- [45] N. Christensen and R. Meyer, Physical Review D **64**, 022001 (2002), gr-qc/0102018.
- [46] C. Rover, R. Meyer, and N. Christensen, *Bayesian inference on compact binary inspiral gravitational radiation signals in interferometric data* (2006), gr-qc/0602067.
- [47] L. Barack and C. Cutler, Physical Review D **69**, 082005 (2004), gr-qc/0310125.
- [48] G. Nelemans, L. R. Yungelson, and S. F. Portegies Zwart, *Astronomy and Astrophysics* (2001), astro-ph/0105221.
- [49] A. J. Farmer and E. S. Phinney, Mon. Not. Roy. Astron. Soc. **346**, 1197 (2003), astro-ph/0304393.
- [50] L. Blanchet, B. R. Iyer, and B. Joguet, Phys. Rev. D **65**, 064005 (2002), Erratum Phys. Rev. D **71**, 129903(E) (2005), gr-qc/0105098.
- [51] T. Damour, B. R. Iyer, and B. S. Sathyaprakash, Phys. Rev. D **63**, 044023 (2001), erratum-ibid. D **72** (2005) 029902, gr-qc/0010009.
- [52] T. Damour, B. R. Iyer, and B. S. Sathyaprakash, Phys. Rev. D **66**, 027502 (2002), *ibid* D **66**, 027502 (2002).
- [53] T. Damour, B. R. Iyer, and B. S. Sathyaprakash, Phys. Rev. D **62**, 084036 (2000), gr-qc/0001023.
- [54] C. Van Den Broeck (2006), gr-qc/0604032.
- [55] C. Van Den Broeck and A. Sengupta (2006), in preparation.
- [56] L. Blanchet, A. Buonanno, and G. Faye (2006), in preparation.